vol. 46, n.° 3, septiembre-diciembre de 2024
ISSN impreso: 0120-0283 • ISSN en línea: 2145-8553

Uplift and denudation of the Antioquia Eastern Massif (Colombia) from fission-tracks thermochronology

Edgar Alland Saenz-Mateus[1, 2*]; Carlos Guillermo Paucar-Álvarez[3]; Jorge Julián Restrepo-Álvarez[4]

[1]Ingeniería de Rocas y Suelos S.A.S.; Medellín, Colombia. (*) esaenz@eafit.edu.co
[2]Escuela de Ciencias Aplicadas e Ingeniería, Universidad EAFIT, Medellín, Colombia.
[3]Departamento de Química, Universidad Nacional de Colombia, Medellín, Colombia. cgpaucar@unal.edu.co
[4]Universidad Nacional de Colombia, Medellín, Colombia. jjrestrepoa@gmail.com

Abstract

Fission-track dating and thermochronology have been used to assess the low-thermal history of some plutonic rocks intruded into the Antioquia Eastern Massif as defined by Gerardo Botero. These techniques enable us to gain a better understanding of the orogenic process that shaped the northern Colombian Central Cordillera. Samples were collected from the Antioqueño Batholith, Sonsón Batholith, and the smaller igneous bodies: La Unión, San Diego, Altavista and Ovejas, all intruded during the Late Cretaceous. Zircon fission track ages vary from 46.4±1.1 Ma to 64.0±1.3 Ma. Mean track lengths are very homogeneous, with variations from 13.9±1.6 µm to 14.6±1.3 µm. The results of thermal annealing modeling carried out with the AFTSolve program show three main segments: 1) Significant decrease in temperature from 240°C to ~50°C in the middle to late Eocene at maximum cooling rates of 50°C/Ma; 2) A period of thermal stability extending into the Middle Miocene; and 3) a final cooling segment through to surface temperature (20°C) at cooling rates of about 4°C/Ma. Results were interpreted as coincident with the Pre-Andean (middle Eocene) and the Eu-Andean (late Miocene-Pliocene) orogenies. This last pulse is related to the recent orogeny that exhumed the analyzed samples, occurring between 3 and 5 Ma ago, interpreted as the maximum time for the formation of the "Central Cordillera" erosion surface and its subsequent superimposed relief. The intermediate quiescent period did not record the Oligocene Proto-Andean orogeny. The tectonic phases produced episodes of uplift and denudational response at maximum rates of 2000 and 160 m/Ma, respectively, using an assumed geothermal gradient of 25ºC/km.

Keywords: Morphogenesis; Andean orogeny; Antioqueño Plateau.

Levantamiento y denudación del Macizo Oriental Antioqueño (Colombia) a partir de termocronología por huellas de fisión

Resumen

Hemos utilizado dataciones y análisis termocronológicos por huellas de fisión para evaluar la historia del enfriamiento de algunas rocas plutónicas emplazadas en el Macizo Oriental Antioqueño definido por Gerardo Botero. Estas técnicas permiten aproximarnos al entendimiento del proceso orogénico que dio forma al actual segmento norte de la Cordillera Central de Colombia. Las muestras usadas provienen del Batolito Antioqueño, del Batolito de Sonsón y de los stocks de La Unión, San Diego,

How to cite: Saenz-Mateus, E.A.; Paucar-Álvarez, C.G.; Restrepo-Álvarez, J.J. (2024). Uplift and denudation of the Antioquia Eastern Massif (Colombia) from fission-tracks thermochronology. *Boletín de Geología, 46*(3), 205-227. https://doi.org/10.18273/revbol.v46n3-2024009

Altavista, Ovejas, todos emplazados durante el Cretácico tardío. Las edades en circones varían entre 46,4±1,1 Ma y 64,0±1,3 Ma. Las longitudes medias de las trazas son muy homogéneas, con variaciones de 13,9±1,6 µm a 14,6±1,3 µm. Los resultados del modelado de recocido térmico realizado con el programa AFTSolve muestran tres segmentos principales: 1) disminución significativa de la temperatura de 240°C a ~50°C en el Eoceno medio a tardío a velocidades máximas de enfriamiento de 50°C/Ma; 2) un periodo de estabilidad térmica que se extiende hasta el Mioceno medio; y 3) un segmento final de enfriamiento hasta la temperatura superficial (20°C) a velocidades de enfriamiento de unos 4°C/Ma. Los resultados se interpretan como coincidentes con las orogenias Preandina (Eoceno medio) y Euandina (Mioceno tardío-Plioceno). La última orogenia, que exhumó las muestras analizadas, se produjo hace 3-5 Ma, edad que se interpreta como la máxima para la formación de la superficie de erosión "Cordillera Central" y su relieve sobreimpuesto. El periodo de quiescencia intermedio no registró la orogenia Protoandina del Oligoceno. Estas fases tectónicas produjeron episodios de levantamiento y respuesta denudativa a tasas máximas de 2000 y 160 m/Ma respectivamente, utilizando un gradiente geotérmico supuesto de 25ºC/km.

Palabras clave: Morfogénesis; Orogenia andina; Meseta antioqueña.

Introduction

Twenty years ago, the master thesis "Fission track thermochronology and denudational response to tectonics in the north of the Colombian Central Cordillera" (Saenz, 2003), was written. A pioneering research for thermochronological studies in the Colombian Andes and a good starting point for many subsequent studies. This thesis was never published, but it has always been a reference for subsequent works, so we believe that its presence in this special bulletin is justified and pertinent.

In recent years, there have been new and important contributions to the knowledge of both thermochronology and the exhumation of the area now called "Antioqueño Plateau" (*e. g.* Toro *et al.*, 2006; Montes-Correa, 2007; Restrepo-Moreno, 2009; Restrepo-Moreno *et al.*, 2009; Villagómez-Díaz, 2010; Noriega-Londoño, 2016; Noriega-Londoño *et al.*, 2020). Reading these articles is essential for understanding the evolution of ideas after this work. In addition, new geochronological and geochemical data have contributed to the knowledge of geological evolution prior to the formation of the relief. For example, data provided by works such as those of Restrepo *et al*. (2011), Villagómez *et al*. (2011), García-Casco *et al*. (2020), Ibáñez-Mejía *et al*. (2020), and others are fundamental to our understanding.

Geological and Geomorphological Framework

Geological Setting

The study area is the Antioquia Eastern Massif (north of the Colombian Central Cordillera), shown in Figure 1, which is composed mostly of metamorphic rocks originated in different pre-cretaceous episodes (*e. g.* Restrepo and Toussaint, 1982; Vinasco *et al.*, 2006; Restrepo *et al.*, 2011; Villagómez *et al.*, 2011), intruded by intermediate to acidic Mesozoic plutons (Aspden *et al.*, 1987; Restrepo and Toussaint, 1990; Leal-Mejía, 2011). This massif represents the northern segment of the Tahamí allochthonous terrane (Restrepo and Toussaint, 2020) bounded at the western flank by ultrabasic rocks with ophiolitic characteristics obducted during Triassic times (*e. g.*, Aspden and McCourt, 1986; Bourgois *et al.*, 1987; García-Casco *et al.*, 2020; Ibáñez-Mejía *et al.*, 2020), and limited to the east by the Chibcha Terrane of continental basement and oceanic sedimentary cover. Thin Cretaceous marine sedimentary sequences and Neogene detritic rocks overlie small areas of the metamorphic and igneous basement. In Figure 2, we only show the studied igneous bodies surrounded by the metamorphic basement and the other units.

This research was focused in the Late Cretaceous intrusives (mainly granodiorites) of which we highlight the Antioqueño Batholith (Feininger and Botero, 1982), whose large area (7221 km^2), geochronological and geochemical variations suggest it is the superposition of different magmas (Leal-Mejía, 2011). Their ages obtained through different methods, vary throughout the Late Cretaceous and even the Paleocene (*e. g.*, Restrepo *et al.*, 2007; Ordóñez *et al.*, 2008; Leal-Mejía, 2011; Villagómez *et al.*, 2011). However, for practical purposes, in this research we will continue to use the term Batholith.

Other intrusives studied include small stocks near the Antioqueño Batholith, like Altavista, San Diego, Ovejas, La Unión, and Sonsón, all of them with Late Cretaceous ages (*e. g.*, Ordóñez-Carmona *et al.*, 2001; Correa *et al.*, 2006) except for the Sonsón Batholith with Paleocene to Early Eocene ages (Leal-Mejía, 2011).

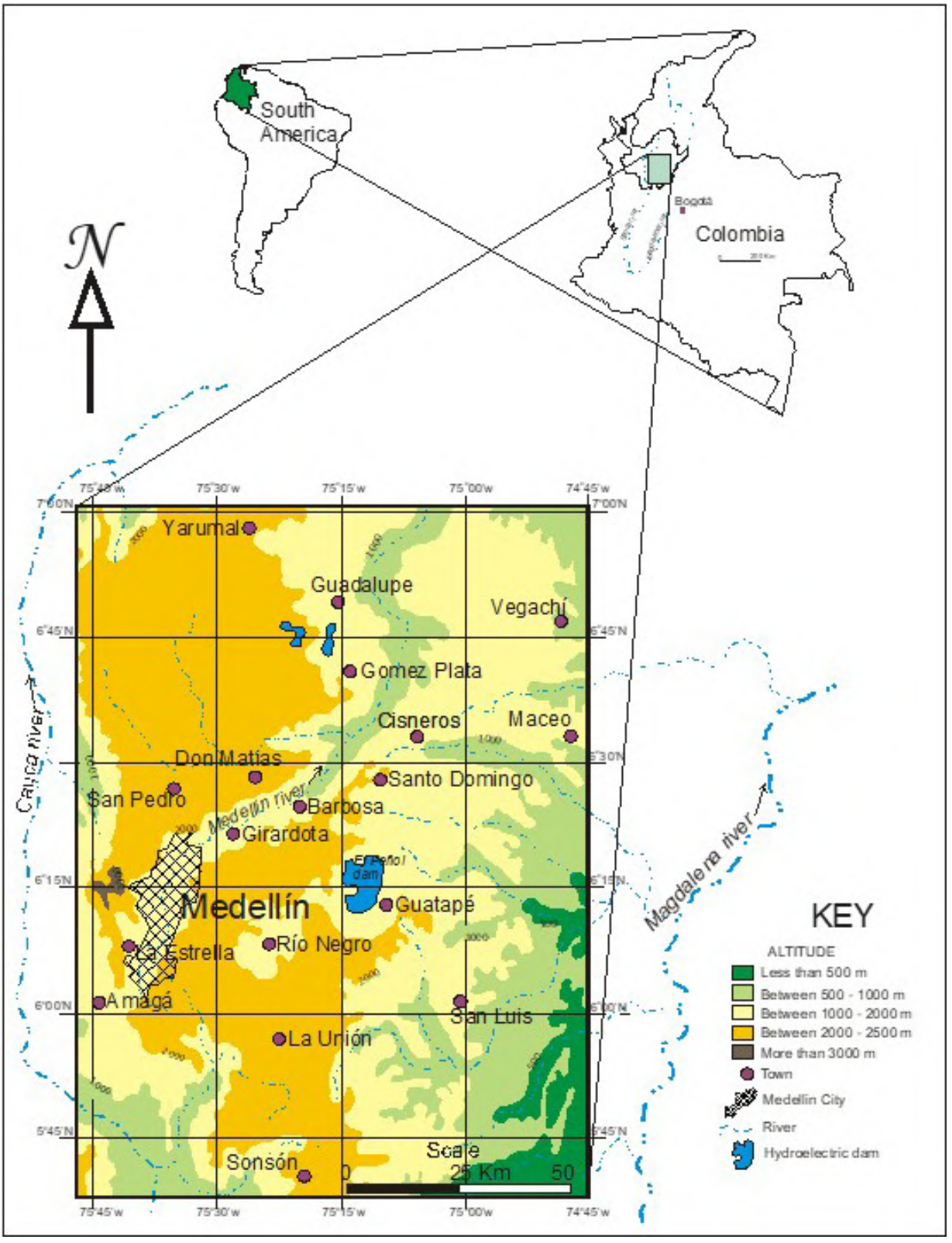

Figure 1. Study area. After SIGAC (2017).

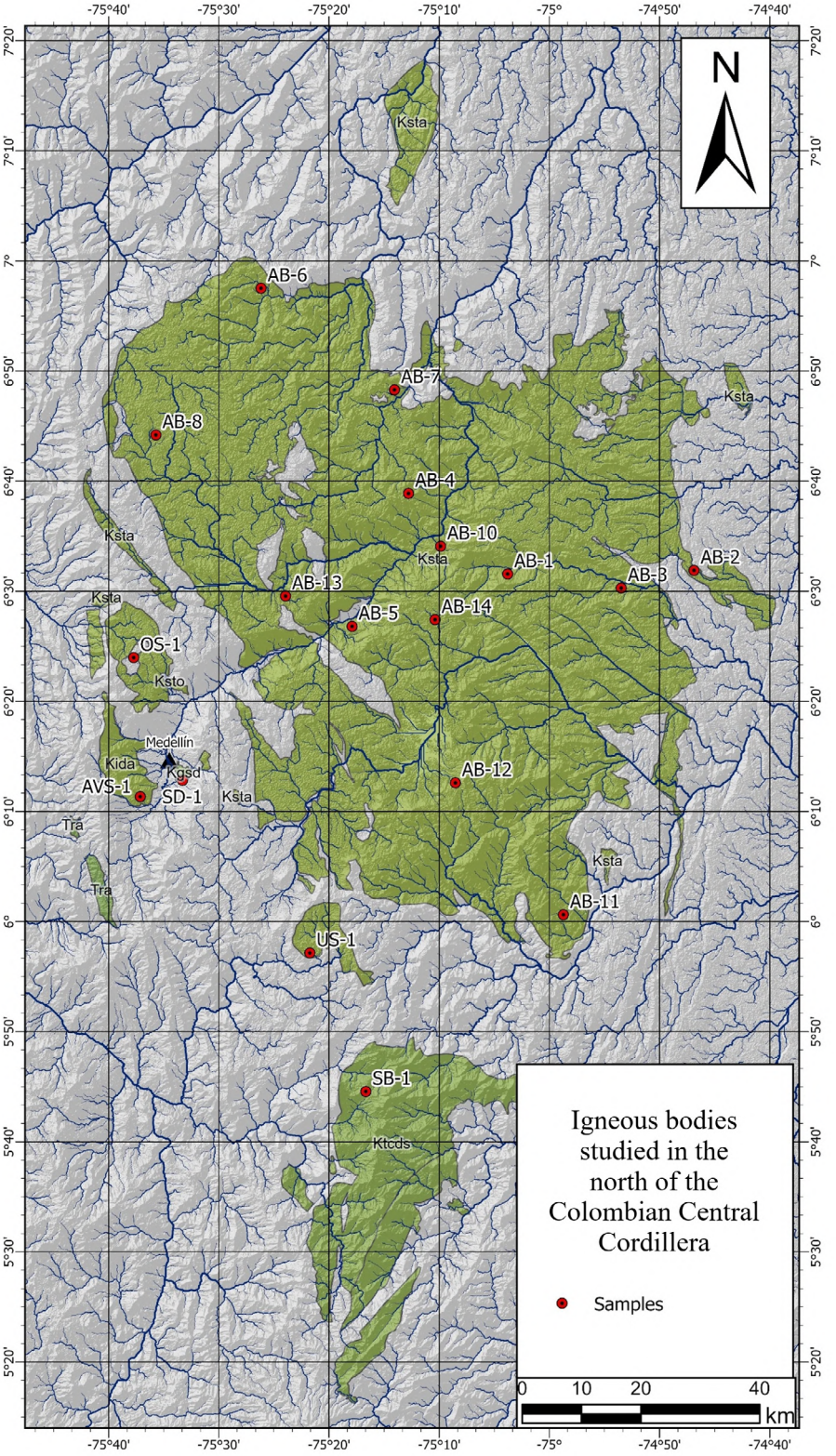

Figure 2. Geological setting. Plutonic units studied (green color) surrounded by undifferenced metamorphic complex (gray color).

Colombian Andes Uplift

The great geological differences among the Colombian cordilleras and their complex geotectonic evolution, as indicated by the exotic terranes theory, suggest a non-homogeneous uplift of the Colombian Andes. For example, the Eastern Cordillera exists as a continuous emerged mountain range only from between 11.8 and 12.9 Ma ago (*e. g.* Hoorn *et al*., 1995), whereas sediments from an uplifted Central Cordillera have been deposited only since Maastrichtian times (Van der Hammen, 1958). In a complex compressive tectonic setting such as the Colombian Andes, several differential or "block uplifts" may have occurred, with different intensities and timing.

The main constraints on the paleogeographic evolution of the Colombian cordilleras have been provided by stratigraphic and paleontological studies, especially palynology. Few radiometric data have been used in the discussion, and geomorphologic features are poorly understood and have not been linked to the tectonic setting.

The first published ideas on the Colombian Andean orogeny (Oppenheim, 1941; Van der Hammen, 1958), concern the stratigraphic studies of the Eastern Cordillera. Van der Hammen concluded that tectonic "orogenetic movements" took place from the beginning of the Maastrichtian and continued at intervals during the Paleogene and Neogene. This gradually shaped the actual form and structure of the Colombian Andes. Table 1 shows the separate phases and subphases into which Van der Hammen divides the Andean orogeny from correlations between stratigraphic information and palynological analysis.

Although the question remains open, as to whether Van der Hammen's approaches are common to the Central and Eastern cordilleras, subsequent regional evolution models (*e. g.*, Irving, 1975; Restrepo and Toussaint, 2020) have introduced few variations to Van der Hammen's model.

Local morpho-tectonic features

To understand the uplift and denudation events that have affected the study area, it is also necessary to understand the "landscape registers" of the geological events. Antioquia Eastern Massif comprises mostly highlands of low relief, which can be recognized as different erosion-surface levels or etchplains separated by erosional scarp slopes and cut by deep canyons. The staggered relief of the northern Central Cordillera is a record of the uplift process, which can be subdivided into several rapid phases that generated the regional erosional scarp slopes and some deep canyons (Page and James, 1981; Arias-López, 1995; Toro *et al*., 2007). Quiescent phases of extremely low tectonic activity occurred in between the uplift phases. These allowed erosion surfaces to develop along with etchplanation near sea level (Büdell, 1982 in Migon, 2006).

This framework allows development of a landscape "relief stratigraphy" in which the main geomorphological features are associated with differential denudation processes that affect the surface in distinct way during episodes of tectonic activity and quiescence. An approximation of the location of these features is shown in Figure 3 and their main characteristics are described below.

Undefined remnants (pre S-I): The oldest flat erosive remnants in the Antioquia Eastern Massif are small areas on the top of the highest mountains. They form a discontinuous belt over the western side of the study area at altitudes between 3000 and 3150 m. Traditionally these have been interpreted as remnants of a poorly preserved etchplain, which has had prolonged exposure to denudation. Page and James (1981) called it Pre-Cordillera Central erosion surface or Pre-S-I and Arias-López (1995) termed it Ancient Highland. However, due to the differences in altitude between the isolated flat areas and the high local tectonic activity, it is not clear whether they were all formed during the same quiescence/denudation morphogenetic episode. Thus, the name of "Undefined Remnants" for this set of morphological units has been suggested (Rendón, 2003).

Table 1. Tectonic orogenic phases of the Colombian Andes as described by Van der Hammen.

Tectonic Phase	Epoch	Subphases
Eu Andean	Miocene and Pliocene	IV - Base of the Pliocene III - Base of the Tortonian II - Base of the Middle Miocene I – Base of the Lower Miocene
Proto Andean	Base of the Upper Oligocene	
Pre Andean	Lower and Mid. Eocene	II – Base of the Middle Eocene I – Base of the Lower Eocene

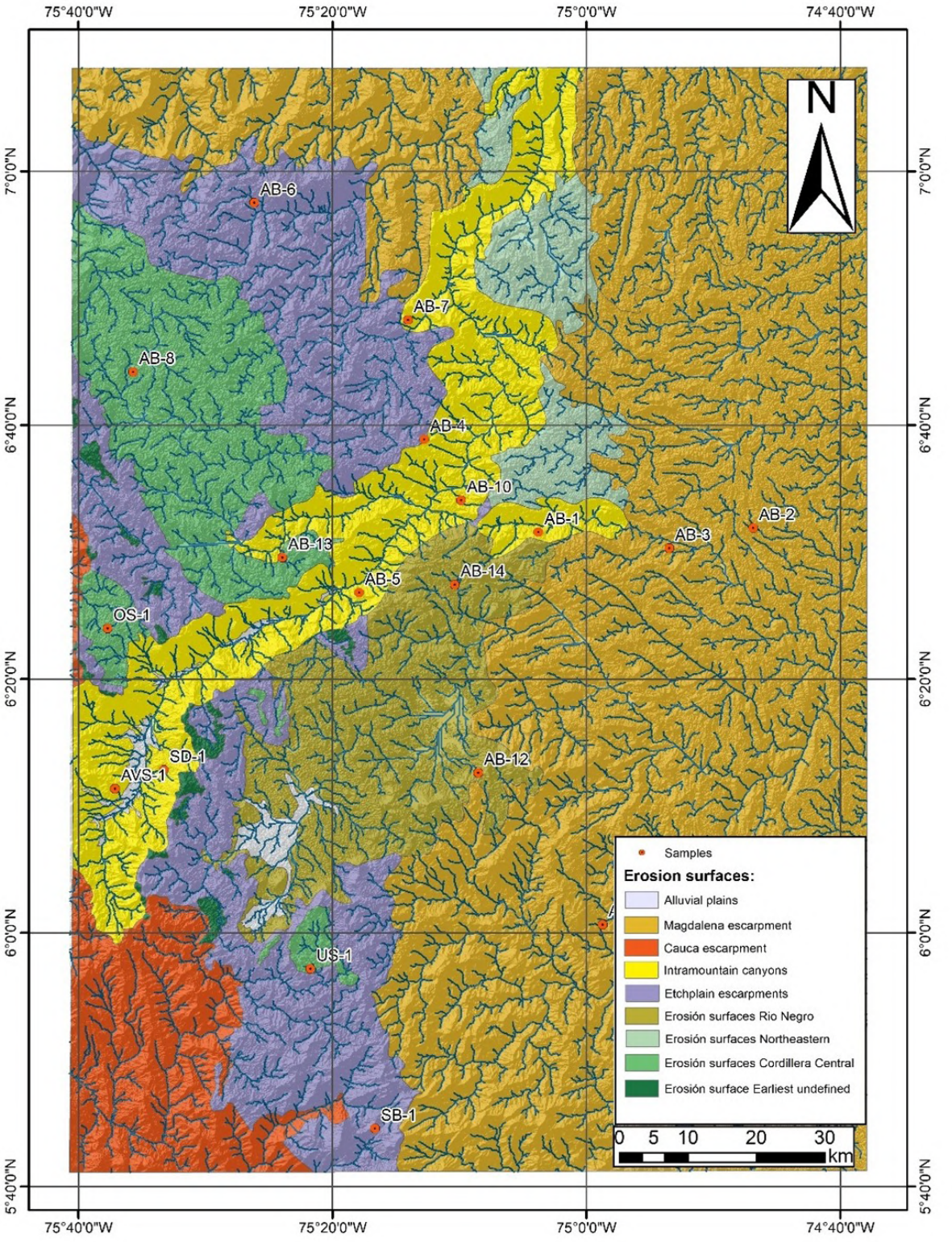

Figure 3. Main morphogenetic unis on the Antioquia Eastern Massif. After Page and James (1981).

Cordillera Central erosion surface (S-I): This feature occurs as low and rounded flat-topped mountains and hills which are wider and better preserved near the range axis. Page and James (1981) called it the Cordillera Central erosion surface or S-I and Arias-López (1995) the Intermediate Highland. These authors differ in their views about the pertinence of the wide Rio Negro area to this surface. Page and James (1981) considered that it corresponds to a different etchplain (S-II), while Arias-López (1995) regarded it as part of the Intermediate Highland. Although we support the first theory, this question remains a matter of debate among specialists.

Rio Negro erosion surface (S-II): The Rio Negro or S-II erosion surface appears as accordant rounded and flat-topped hills dissected by short streams, located 200 to 400 m below the Cordillera Central erosion surface, and better preserved (Page and James, 1981).

Northeastern erosion surface: This etchplain was defined by Arias-López (1995) in the northeast of the study area. He named it the Inferior Highland and divided it in three segments: Carolina-Gomez Plata, Anorí, and Amalfi-Yolombó highlands. It forms flat to rounded hills at an altitude of about 1500 m, with eastward dip.

Erosional scarp slopes: After each surface erosion uplift, the denudation process began to act over it. Denudation is initially more intense on the edges and gradually destroys the uplifted terrane to form a new erosion surface. While that process is being conducted, an intermediate zone forms between the newly created surface and the older one. That zone is an erosional scarp slope, at which there are deep streams, steep slopes, and older remnants, among others features of highly active denudation landscapes. In the study area at least two of them can be recognized between the above noted erosion surfaces.

High-active erosion escarpments (Cauca and Magdalena): The largest Colombian intermontane streams are the Cauca River, which separates the Western and Central Cordilleras, and the Magdalena River, which divides the Central and Eastern Cordilleras. Between their axis and the erosion surface edges there are intensive denudation flanks and erosion escarpments.

Intermontane Canyons: Sharp and deep canyons cut the older erosion surfaces and the etchplain escarpments. This development is associated with denudation and tectonic movements. The Medellin-Porce River and Nus River canyons stand out in the study area. The former is especially interesting, since it contains a peculiar tectonic anomaly (Hermelin, 1982) called Aburrá Valley, probably with an associated pull-apart genesis (Rendón, 2003).

Fission-track Methods

Apatite Fission Tracks Analyses

Fission track analyses have proved to be a successful and sensitive thermochronometer to reconstruct the thermal histories of the geologic units studied. This technique is widely known in the literature as AFTT (Apatite fission track thermochronology) and reports the trajectory of the sample between the time it passed through the 110±10°C isotherm (normally the upper 4 km of the crust) and the surface. AFTT reveals the magnitude and timing of each thermal episode. Understanding of their nature and causes are the keys for any geological interpretation. Reheating over 120°C completely anneals the tracks, and the thermal history path shows information only about the last cooling. Overheating below 110°C can be detected, although the accuracy of those trends is poorer than in the case of simple cooling episodes (Gleadow and Brown, 1999). Therefore, the AFTT records cooling and quiescence episodes, most of which correspond to tectonic disturbances and their denudational responses.

Thermal histories modelling

Modeling of time-Temperature paths of five samples from the Antioqueño Batholith and one sample from the Sonsón Batholith was carried out using the AFTSolve (version 1.2.2© 2001 Donelick Analytical, Inc. and Richard A. Ketcham) program which provides thermal histories considering the variability of apatite fission tracks annealing kinetics (Carlson *et al*., 1999; Donelick *et al*., 1999; Ketcham *et al*., 1999). To run it, for each grain used it was necessary to input: age, standard deviation, track length, angle with the c-axis, and Cl content.

The annealing model (multikinetic), the kinetic parameter (Cl), the modeling scheme (Montecarlo), the half segments (*i. e*., divisions of the t-T paths, 5), and the number of paths to generate randomly (30000) were selected. The AFTSolve program takes each candidate t-T path and generates its respective track-length distribution, which is compared to the measured distribution. The goodness of fit was evaluated with the Kolmogorov-Smirnov (K-S) statistical test, which determines the probability that a set of samples taken

randomly from the known distribution would have a greater maximum separation from it on a cumulative distribution function plot (an ordering of track lengths) than is observed for the sample distribution being tested.

AFTSolve solutions present a best-fit t-T path with two envelopes, the wider envelope in green (acceptable fit) contains all t-T paths that have a K-S of at least 0.05 (5%), and the second purple envelope (good fit) marks the limit of statistical precision, containing all t-T paths that have a merit function value of at least 50%. The goodness of fit for the age (Age GOF) is determined in an analogous way, if the measured age and standard deviation describe a normal distribution. Again, the limit of statistical precision is 50% (Age GOF=0.5).

Samples

Nineteen samples from plutonic rocks were collected and analyzed. These were taken from insitu outcrops of roads and rivers to obtain non-altered material. Table 2 and Figure 2 show their position.

Table 2. Sample's location.

Code	Geological body	Description	Latitude North	Longitude East	Altit. (m)
AB-1	Antioqueño batholith	Coarse-grained hornblende-biotite-granodiorite with phaneritic texture	6º32'16''	75º04'43''	1025
AB-2	Antioqueño batholith	Coarse-grained biotite-granodiorite with seriate texture	6º33'12''	74º47'28''	980
AB-3	Antioqueño batholith	Coarse-grained biotite-granodiorite with phaneritic texture	6º30'48''	74º54'48''	870
AB-4	Antioqueño batholith	Coarse-grained biotite-hornblende-granodiorite with seriate inequigranular and graphic textures	6º39'58''	75º13'31''	1850
AB-5	Antioqueño batholith	Coarse-grained biotite-hornblende tonalite with phaneritic texture	6º27'30''	75º18'18''	1280
AB-6	Antioqueño batholith	Coarse-grained hornblende-biotite granodiorite with seriate inequigranular texture	6º58'36''	75º26'13''	2100
AB-7	Antioqueño batholith	Coarse-grained biotite-granodiorite hiatal inequigranular texture	6º48'05''	75º13'15''	1027
AB-8	Antioqueño batholith	Coarse-grained biotite-hornblende granodiorite with large grains, most of them of hypidiomorphic texture	6º44'14''	75º35'55''	2650
AB-9	Antioqueño batholith	Coarse-grained hornblende-biotite granodiorite Locally shows myrmekitic and flow textures	6º24'40''	75º24'40''	1500
AB-10	Antioqueño batholith	Coarse-grained biotite-granodiorite with seriate inequigranular texture	6º37'08''	75º09'24''	1050
AB-11	Antioqueño batholith	Coarse-grained hornblende granodiorite with granophyric, local myrmekitic and graphic textures	6º02'41''	75º00'09''	1075
AB-12	Antioqueño batholith	Coarse-grained monzogranite with seriate inequigranular texture	6º13'31''	75º09'00''	1950
AB-13	Antioqueño batholith	Coarse-grained biotite-hornblende tonalite Alteration is common as well as fractures due to weathering	6º30'53''	75º24'53''	2200
AB-14	Antioqueño batholith	Coarse-grained hornblende granodiorite with seriate grain distribution	6º30'06''	75º13'35''	1900
SB-1	Sonsón batholith	Coarse-grained hornblende-biotite granodiorite with phaneritic inequigranular texture	5º46'10''	75º18'05''	2250

Continued Table 2.

Code	Geological body	Description	Latitude North	Longitude East	Altit. (m)
US-1	La Unión Stock	Coarse-grained biotite tonalite with alteration and tectonic texture	5º56'00''	75º18'25''	2420
SD-1	San Diego Stock	Pegmatitic hornblende gabbro	6º13'02''	75º33'38''	1850
AV-1	Altavista Stock	Fine-grained granodiorite with inequigranular texture	6º12'23''	75º40'13''	1840
OS-1	Ovejas Stock	Coarse-grained biotite-granodiorite	6º21'56''	75º36'16''	2450

Results

Zircons Fission Tracks dating

The external detector method for fission track dating was followed in this project. Analyses were made using a geometry factor of 1/2, and the chi-squared (x^2) test was applied to determine the degree to which individual grain ages belong to a simple population age (Galbraith, 1981). The ages were determined using the zeta (ζ) calibration method (Hurford and Green, 1983) with a value of 374.36±4.76, weighted according to uncertainties on six individual z-values. Zircon ages are summarized in Table 3 as central ages (Galbraith and Laslett, 1993) with a ±1σ error. Information displayed in the tables also includes the densities of the spontaneous (ρs), induced (ρi) and glass monitor (ρ_M) tracks. Ns, Ni and N_M are the number of tracks counted. The software TrackKey version 4.1® (Dunkl, 2002), was used for data processing.

Table 3. Zircon Fission Track Ages.

Sample	No. of crystals	Spont. tracks		Ind. tracks		Glass monitor		P(x^2) %	Central age±1σ (Ma)
		ρs (10^5 cm^{-2})	Ns	ρi (10^5 cm^{-2})	Ni	ρ_d (10^4 cm^{-2})	N_d		
AB-1	20	30.81	9875	18.08	5795	15.28	6683	23.6	46.4±1.1
AB-2	16	54.88	9955	27.78	5039	15.28	6683	21.7	53.8±1.2
AB-3	21	38.03	5343	21.42	3009	15.28	6683	96.2	48.3±1.2
AB-4	19	35.35	13953	18.41	7266	15.28	6683	27.7	52.3±1.0
AB-5	23	35.64	7081	20.48	4070	15.28	6683	95.8	47.4±1.1
AB-6	14	50.26	20248	21.26	8566	15.28	6683	6.3	64.0±1.3
AB-7	19	47.20	11867	20.14	5064	15.28	6683	98.7	63.7±1.3
AB-8	20	54.74	10849	26.62	5277	15.28	6683	17.0	55.9±1.2
AB-9	21	46.03	18753	24.49	9979	15.28	6683	37.8	51.1±0.9
AB-10	21	33.10	10384	16.45	5160	15.28	6683	77.6	54.7±1.2
AB-11	13	51.11	6537	22.49	2876	15.28	6683	90.6	61.8±1.6
AB-12	16	56.17	9004	27.54	4414	15.28	6683	73.4	55.5±1.2
AB-13	20	40.93	8367	26.60	5437	18.85	7659	92.9	51.7±1.1
AB-14	20	43.15	11426	24.80	6566	15.28	6683	33.5	47.4±0.9
SB-1	22	44.77	15713	25.13	8822	15.28	6683	12.6	48.6±1.0
US-1	21	120.80	5643	56.70	2648	15.28	6683	24.8	58.0±1.7
SD-1	7	61.02	7121	28.05	3273	15.28	6683	36.3	59.3±1.5
AV-1	7	178.90	4151	103.40	2398	18.85	7659	13.6	58.5±2.0
OS-1	20	72.04	12088	34.22	5742	15.28	6683	98.1	57.3±1.2

All zircon data pass the P(x^2)-test at the 5% criterion, indicating that the variability in the track count data is limited to the inherent variability of the fission decay process. Nineteen samples have Paleogene ages ranging from 46.4±1.1 Ma to 64.0±1.3 Ma.

Thermal history analyses

Time-temperature (T-t) paths were generated for the six representative samples shown in Figure 5 to Figure 10. They were generated between two constrained points: the present surface temperature at 20°C, and the zircon fission track age, which has a closure temperature of 240±50°C (*e. g.*, Hurford, 1986).

For thermal history analysis, only the use of apatites is applicable. Unfortunately, not all the samples contained enough confined tracks for the length measurements studies, only nine samples had suitable apatites for measurement. Of these, six samples were modeled.

***Chemical Composition*:** To determine the variability of the annealing kinetics and evaluate the dependency of single grain age and length distribution on the chemical variation, the chemical composition was determined both for each grain where a confined track was detected, and for each grain where the age was calculated.

The analyses were made with an electron probe microanalyser (EPMA) JEOL JXA-8800, using carbon coating, accelerating voltage of 15 kV, probe current $2.5x10^{-8}$ A and a probe diameter of 20 µm. Durango apatite was used as a standard to determine the fluorine content, and chlorine-rich potassium hastingsite from Ongul Island (Suwa *et al.*, 1987) was used to determine the chlorine content. The other major chemical components of the apatites were determined using synthetic standards. The results for each sample are summarized in Table 4, showing the average, maximum and minimum value in wt% for its major components, taking into account the generic composition $Ca_5(PO_4)_3(OH,F,Cl)$.

Chlorine content (Cl wt%) was the kinetic parameter employed to determine the difference in annealing resistance due to its negligible variations within samples; this can be appreciated in the CaO *vs* Cl (Figure 4) variation diagrams. The kinetic population used in each analysis is the arithmetic mean of the individual measurements per sample. Fluorine contents are much greater than chlorine and display wider variation.

Table 4. Chemical composition of the analyzed apatites (wt%).

Sample	# of Grains		Na_2O	SiO_2	Al_2O_3	CaO	FeO	Cl	F	P_2O_5	Total
AB-1	60	Average	0.070	0.012	0.007	51.499	0.027	0.127	3.661	41.611	97.015
		Max	0.389	0.150	0.066	53.399	0.105	0.294	3.852	43.075	99.119
		Min	0.009	0.000	0.000	48.406	0.000	0.086	3.485	39.504	93.071
AB-6	83	Average	0.041	0.048	0.004	51.791	0.040	0.220	3.657	42.051	97.845
		Max	0.179	0.130	0.041	53.896	0.149	0.676	3.799	43.011	99.771
		Min	0.000	0.000	0.000	49.668	0.000	0.151	3.476	39.984	93.636
AB-7	82	Average	0.089	0.083	0.007	50.733	0.121	0.610	3.586	41.403	96.682
		Max	0.152	0.267	0.090	53.265	0.282	0.918	3.797	42.614	99.136
		Min	0.029	0.000	0.000	48.063	0.013	0.413	3.303	38.511	91.992
AB-9	52	Average	0.036	0.088	0.005	52.414	0.024	0.129	3.660	41.031	97.388
		Max	0.140	0.176	0.040	54.607	0.083	0.259	4.290	42.340	100.661
		Min	0.000	0.000	0.000	48.325	0.000	0.019	2.601	37.228	90.274
AB-13	92	Average	0.037	0.160	0.014	51.520	0.042	0.392	3.569	41.433	97.167
		Max	0.443	0.684	0.250	54.430	0.170	0.502	3.806	43.519	101.724
		Min	0.000	0.007	0.000	44.911	0.000	0.210	2.758	35.036	84.129
SB-1	73	Average	0.084	0.111	0.003	51.328	0.067	0.166	3.673	41.593	97.025
		Max	0.349	0.359	0.027	52.239	0.159	0.405	3.974	42.427	98.192
		Min	0.010	0.000	0.000	48.507	0.000	0.092	3.112	39.395	93.178

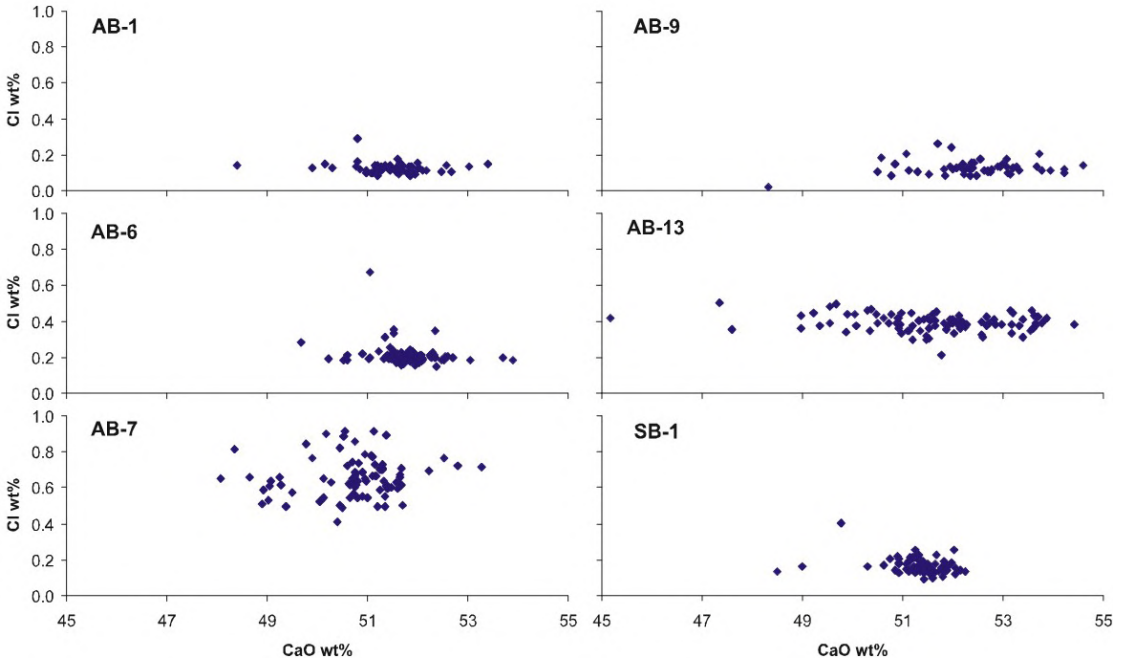

Figure 4. Harker diagram showing variation of Cl according to CaO (wt%).

Thermal history modeling: The thermal history figures are schematically complemented with U-Pb zircon ages of 82±8 to 98±27 Ma for the Antioqueño Batholith (Ordóñez-Carmona and Pimentel, 2001) and 73±9 to 55.8±1.0 Ma for the Sonsón Batholith (Ordóñez-Carmona *et al*., 2001; Leal-Mejía, 2011). An additional constraint is given by K/Ar-biotite ages for samples AB-7, AB-13, and SB-1. Samples from the same sites as those in this study were dated with that method, yielding respective ages of 70.6±3.1 Ma to 80.8±3 Ma (Botero-Arango, 1963; Pérez-Ángel, 1967). These data were recalculated using constants of Steiger and Jager (1977). K/Ar-biotite dating represents a closure temperature of 300±50°C (Hurford, 1986).

Modeling of the six samples (Figure 5 to Figure 10) generated segmented time-temperature histories of similar shapes, characterized by marked decrease in temperature at the beginning of the cooling path, a stage of thermal stability, and final cooling until the surface temperature. These paths have been derived of homogeneous mean-track lengths, which vary from 13.9±1.6 µm to 14.6±1.3 µm, ss shown in the histogram that accompanies each of the cooling curves. Characteristics of the model generated for each sample are described below.

Determination of the denudation rates: According with the local geotectonic history, the non-linear thermal histories of the samples (Figure 5 to Figure 10) are a direct consequence of the denudation and uplift processes that affected the study area. Estimation of denudation rates based on apatite fission track thermochronology is a long-term approach. A complete study to define rates of erosion and uplift requires interdisciplinary research that also would include tectonics, stratigraphy, geomorphology, geophysics, low- temperature thermochronometers (*e. g.* as cosmogenic rays) and numerical modeling. The solutions presented herein are only a part of such work.

Conversion of cooling rates to denudation rates requires knowledge of the geothermal gradient over time and the geological environment in which the samples cooled. Denudation rates are here calculated from the ratio *Cooling rate/Geothermal gradient*, which provides a long-scale solution for the different segments of the cooling paths revealed by the apatite fission track annealing model.

No information on heat flow or temperature variations with depth is available for the study area, therefore a sensitivity analysis was performed. Table 5 lists the denudation rates calculated according to the different geothermal gradients that could be expected (20, 25, 30 and 35°C/km).

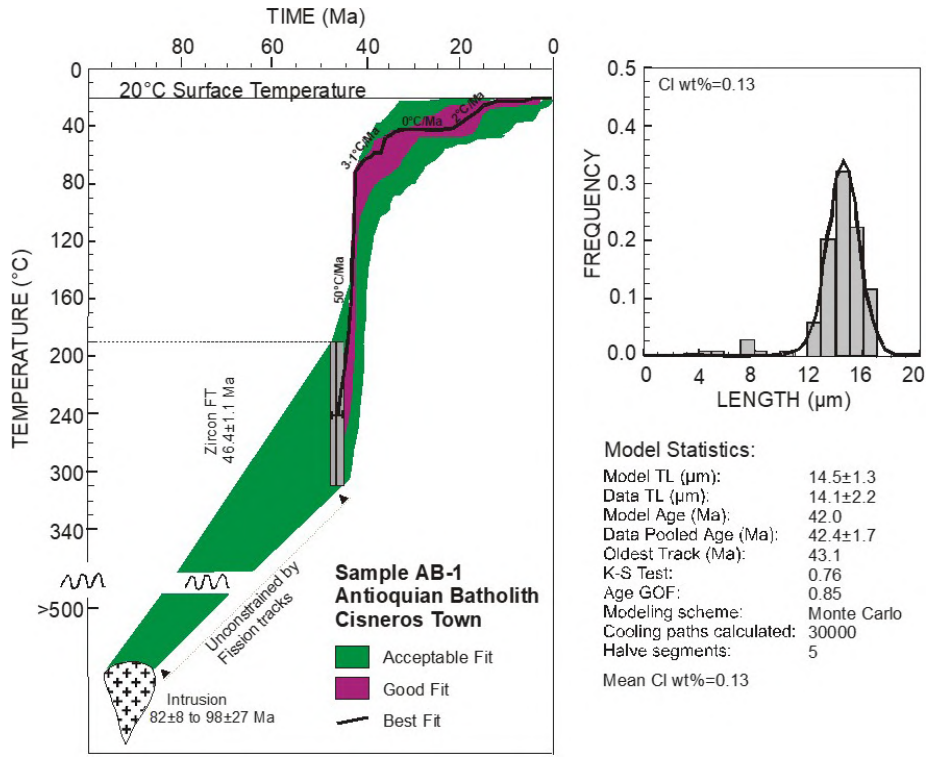

Figure 5. T-t path for sample AB-1.

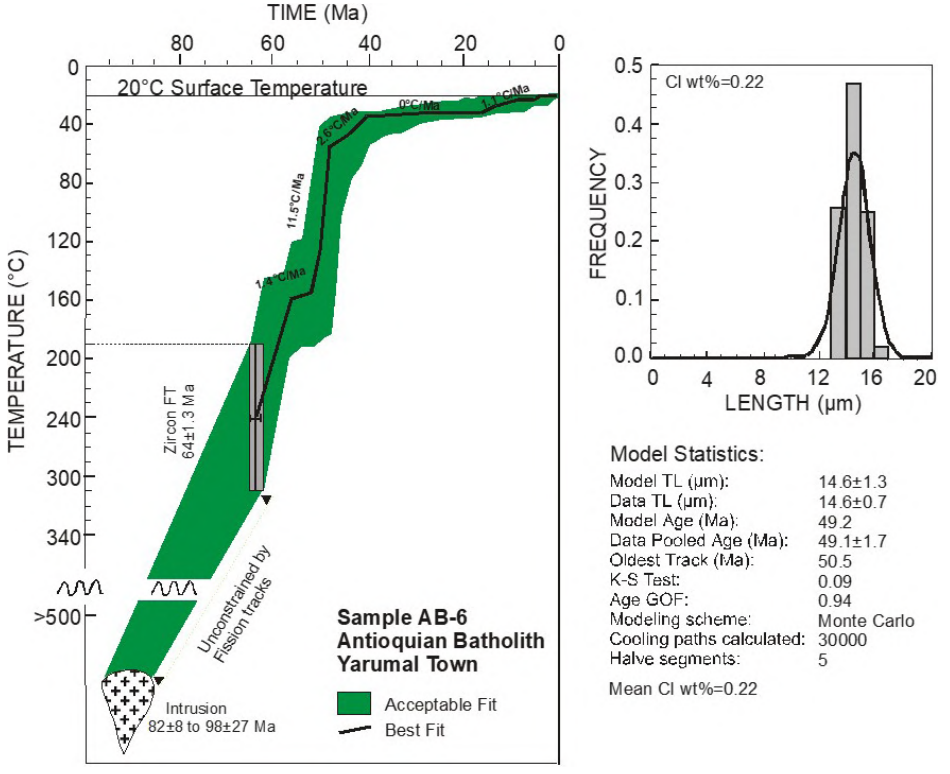

Figure 6. T-t path for sample AB-6. Here the software did not find an area of good fit.

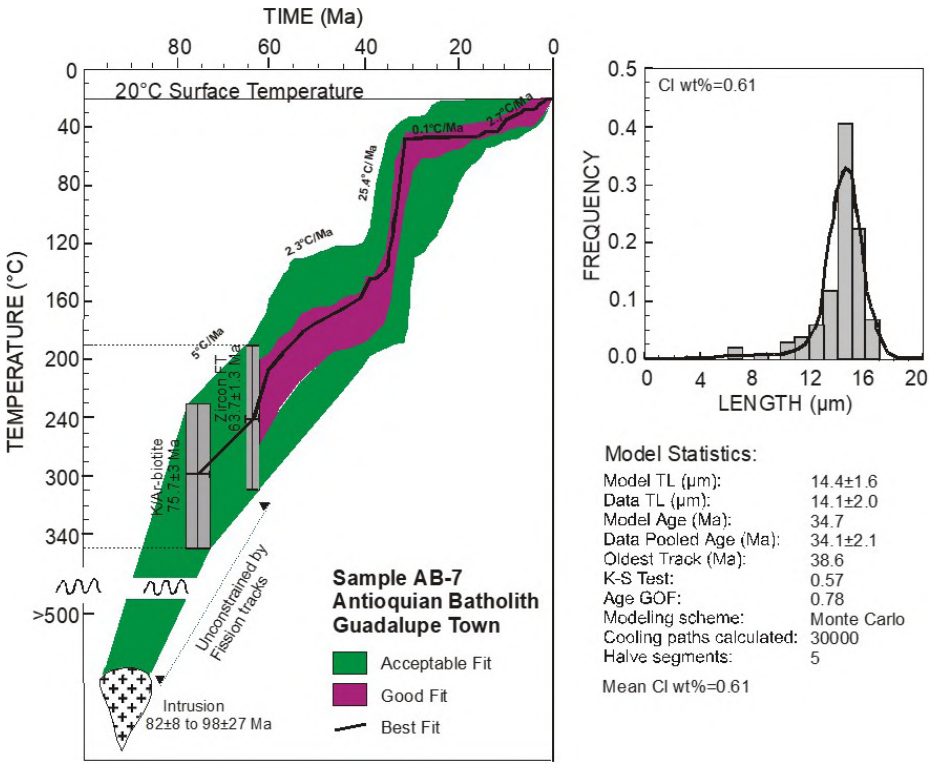

Figure 7. T-t path for sample AB-7.

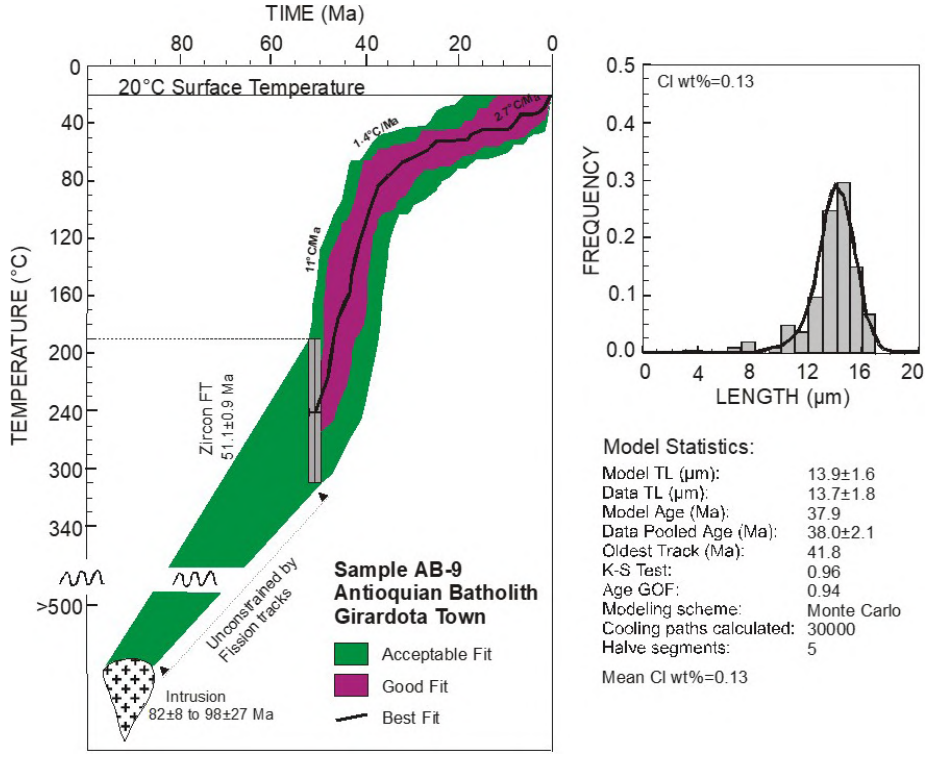

Figure 8. T-t path for sample AB-9.

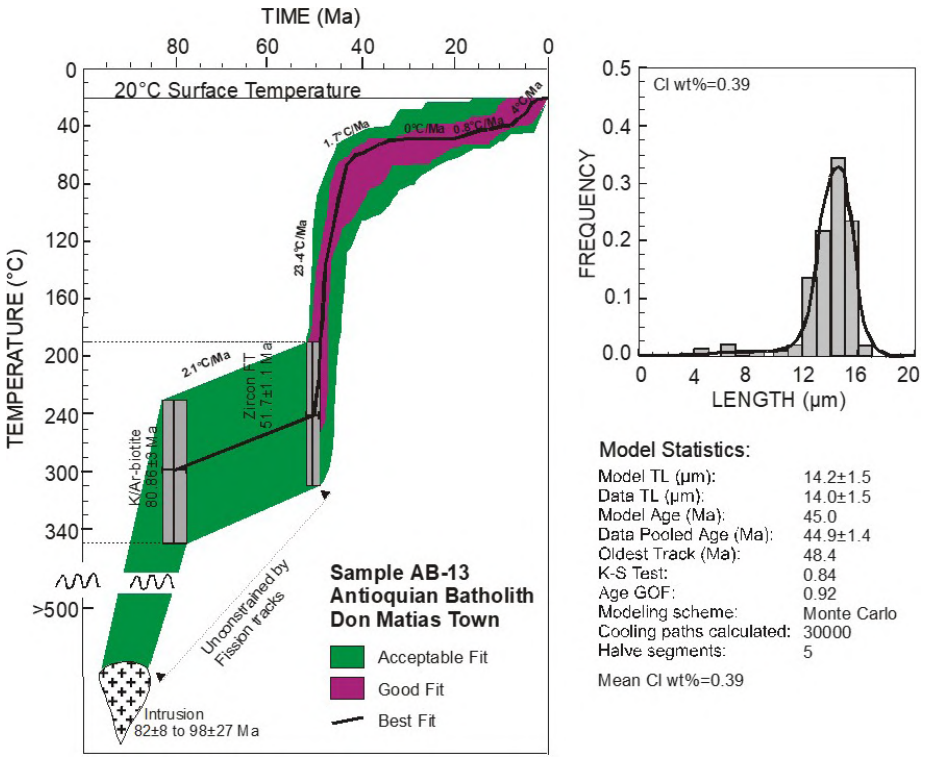

Figure 9. T-t path for sample AB-13.

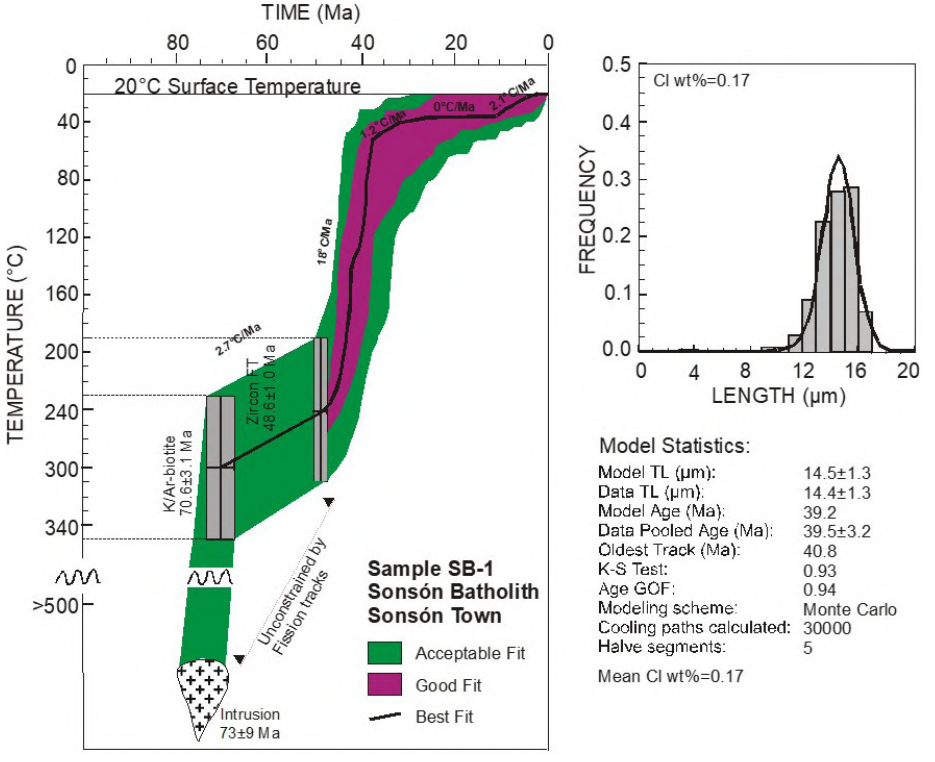

Figure 10. T-t path for sample SB-1.

Table 5. Denudation rates according to the geothermal gradient.

Sample	Stages of constant cooling			Denudation rate (m/Ma)			
	Beginning (Ma)	End (Ma)	Cooling rate (°C/Ma)	Using 20°C/km	Using 25°C/km	Using 30°C/km	Using 35°C/km
AB-1	46.4	43	50.0	2500	2000	1667	1429
	43	34	3.1	155	124	103	89
	34	22	0	0	0	0	0
	22	12	2.0	100	80	67	57
	12	5	0.3	15	12	10	9
AB-6	64	48	11.5	575	460	383	329
	48	41	2.6	130	104	87	74
	41	17	0	0	0	0	0
	17	5	1.1	55	44	37	31
	5	0	0	0	0	0	0
AB-7	63.7	53	5	250	200	167	143
	53	35.5	2.3	115	92	77	66
	35.5	32	25.4	1270	1016	847	726
	32	12	0.1	5	4	3	3
	12	3	2.7	135	108	90	77
AB-9	51.1	37	11.0	550	440	367	314
	37	9	1.4	70	56	47	40
	9	0	2.7	135	108	90	77
AB-13	51.7	43	23.4	1170	936	780	669
	43	34	1.7	85	68	57	49
	34	20	0	0	0	0	0
	20	8	0.8	40	32	27	23
	8	3	4.0	200	160	133	114
SB-1	48.6	38	18.0	900	720	600	514
	38	27	1.2	60	48	40	34
	27	12	0	0	0	0	0
	12	4	2.1	105	84	70	60

Discussion

Interpretation of Zircon FT ages

All Zircon FT dates show statistical homogeneity and can be interpreted as cooling ages, indicating the time at which the sample passed through its closure temperature, estimated to be about 240°±50°C (*e. g.*, Hurford, 1986).

The Antioqueño Batholith occupies most of the study area, and the 14 ages determined range from 46.4±1.1 Ma to 64.0±1.3 Ma. A plot of these data against their present altitude (Figure 11) shows that there is no relationship between the zircon FT ages and topographic position of the samples. Therefore, these ages are not dependent on surface processes such as denudation or block faulting.

Instead, it is apparent that the younger ages are in the center of the body, and ages increase gradually toward the edges of the pluton, as shown in Figure 12 from a simple linear interpolation done by the Surfer software, with the equal age band. This suggests that the zircon fission track ages are linked to normal conductive heat loss of the Antioqueño Batholith, following a radial pattern from inside outwards, between early Paleocene and middle Eocene. This relaxed setting could result from two causes: a tectonically undisturbed quiescent period or a slow and homogeneous surface uplift of the mountain range during those times.

For the other plutons studied, statistical homogeneity of the data and topographic independence of the ages is also clear. The zircon FT age of 48.6±1.0 Ma for the Sonsón batholith is the youngest of the studied plutons. That sample was collected from the northern edge of the pluton, and thus could represent the endpoint of the zircon fission track decay system of that unit. This date supports that the Sonsón Batholith is somewhat younger than the Antioqueño Batholith (Ordóñez-Carmona *et al*., 2001; Leal-Mejía, 2011).

Zircon FT ages of the Ovejas (57.3±1.2 Ma), San Diego (59.3±1.5 Ma), Altavista (58.5±2.0 Ma) and La Union (58.0±1.7 Ma) stocks are similar, with values close to the average age of the Antioqueño Batholith. Interpretation in terms of cooling ages is difficult, since the small size of these units would permit faster heat loss relative to the main Antioqueño Batholith body.

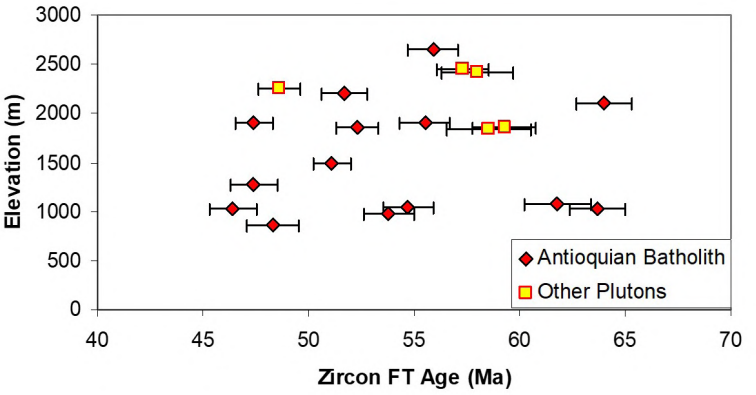

Figure 11. Variation of zircon FT age relative to the elevation of the sample.

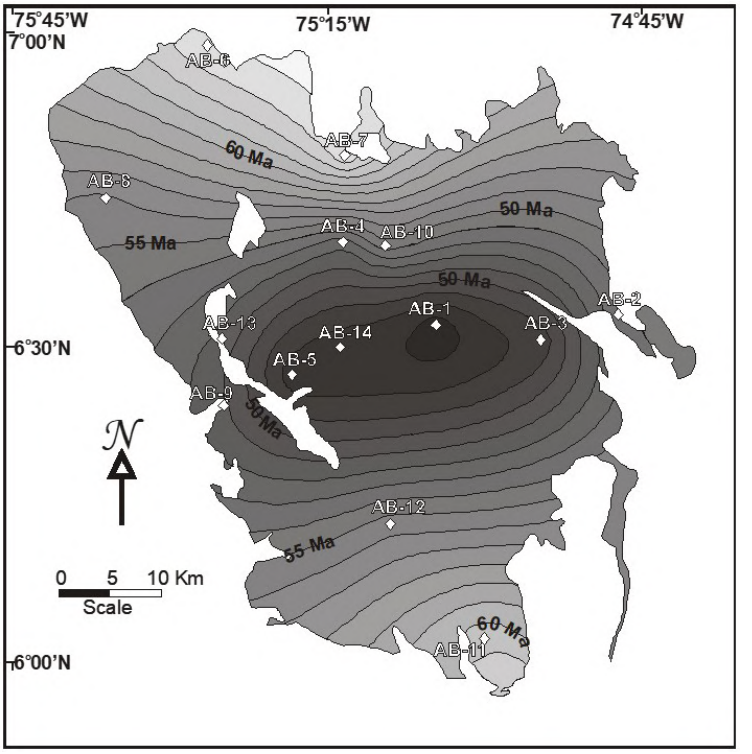

Figure 12. Distribution and variation of zircon FT ages in the Antioqueño Batholith.

Interpretation of the thermal history modeling

The t-T paths generated herein (Figure 5 to Figure 10) are strongly linked to those orogenic phases, especially to those which occurred during the middle Eocene, late Miocene, and Pliocene. The Oligocene phase (proto-Andean) was not captured by the apatite fission track thermochronology modeling probably because the intensity and duration of that episode was insufficient to affect the track length distribution, or simply because the uplift produced in the study area during Oligocene was negligible. Paleogeographic models at that time (*e. g.*, Villamil, 1999) suggest stronger southern uplift and northern collapse of the Central Cordillera. The study area is located near the midway point; thus, the second explanation may be more appropriate. In any case, it must be emphasized that apatite AFTT is an isolated tool that should be used in conjunction with many other disciplines to derive accurate models for the Andes development.

For all t-T paths generated, the stronger cooling episode shows marked coincidence with the pre-Andean orogeny, which reached its climaz in the middle Eocene. This uplift caused a pronounced regional angular unconformity in the Magdalena Valley and Eastern Cordillera, with an important decrease in the regional accommodation space (*e. g.*, Duque-Caro, 1980). The presence of isolated pockets of molasse units in the Magdalena Valley (such as the Pocará and Hoyón Formations) derived from the Central Cordillera suggest an accelerated uplift rate of this Cordillera during the middle Eocene orogenic event (Villamil, 1999).

Eastward migration of the Eastern Cordillera depocenter during the middle Eocene suggests that the deformation front of the orogeny propagated eastward, affecting the western regions more abruptly than the eastern side (Villamil, 1999). The t-T paths modeled also confirm this observation. A plot of the cooling paths from west to east shows that the western samples cooled earlier than the eastern ones. Figure 13 clearly shows such migration in relation to the climax of the pre-Andean phase. The westernmost sample (AB-6) was affected by an earlier pulse before the orogenic peak, whereas the easternmost sample (AB-7) registered the uplift almost 15 Ma later. The relation among these samples is only erosive, as they belong to the same tectonic block and lack intervening faults that could obscure the analysis.

After the pre-Andean orogeny, the sedimentary record of the Magdalena Valley and Eastern Cordillera record a quiescent period that allowed subsidence and marine transgression. During the late Eocene, these sites received sediments from the Central Cordillera (*e. g.*, Anderson, 1972), until interruption by the Oligocene uplift (proto-Andean orogeny).

The middle Miocene and Pliocene epochs are times of major uplift phases in the building of the Colombian Andes and other regions of the world. One of the peaks of the Eu-Andean orogeny coincides with the major worldwide NH3 hiatus dated at 12.9 to 11.8 Ma (Keller and Barron, 1987), and with dramatic paleogeographic changes in the history of the northern Andes (*e. g.*, Hoorn *et al.*, 1995). Other peaks could support the idea for final closure of the Panama isthmus between 7 and 3.1 Ma (Duque-Caro, 1990). The Eu-Andean orogeny is well represented in the generated cooling paths; however, this case, there is no trend in relation with the deformation front (Figure 13).

Implications for the local geomorphology

The late Miocene to Pliocene Eu-Andean orogeny brought all samples to the surface temperature (20°C) between 5 and 3 Ma according to the best-fit line. However, considering the 50% goodness of fit (the limit of the statistical precision), exhumation could have occurred after the last 11 Ma. These ages can be interpreted as maximums for the formation of the current geomorphological features of the Antioquia Eastern Massif.

The late Miocene-Pliocene ages determined here contradict those proposed by Page and James (1981). Based on indirect extrapolations of ^{14}C and paleomagnetic data combined with geomorphological observations, those authors suggest a late Oligocene or early Miocene age for the S-I erosion surface.

The prolonged period of stability between the late Eocene and the middle Miocene revealed by the cooling paths, must have allowed a prolonged planation. The resultant erosion surface after that planation was uplifted during the Eu-Andean orogeny and was destroyed by the intense climatic and tectonic activity which followed. The question if the highest geomorphologic expressions that crop out in the study area (termed here *undefined remnants*) were formed during that planation period, or if they are the result of isolated uplifted blocks, must be solved with additional information, problem also addressed by Noriega-Londoño *et al.* (2020).

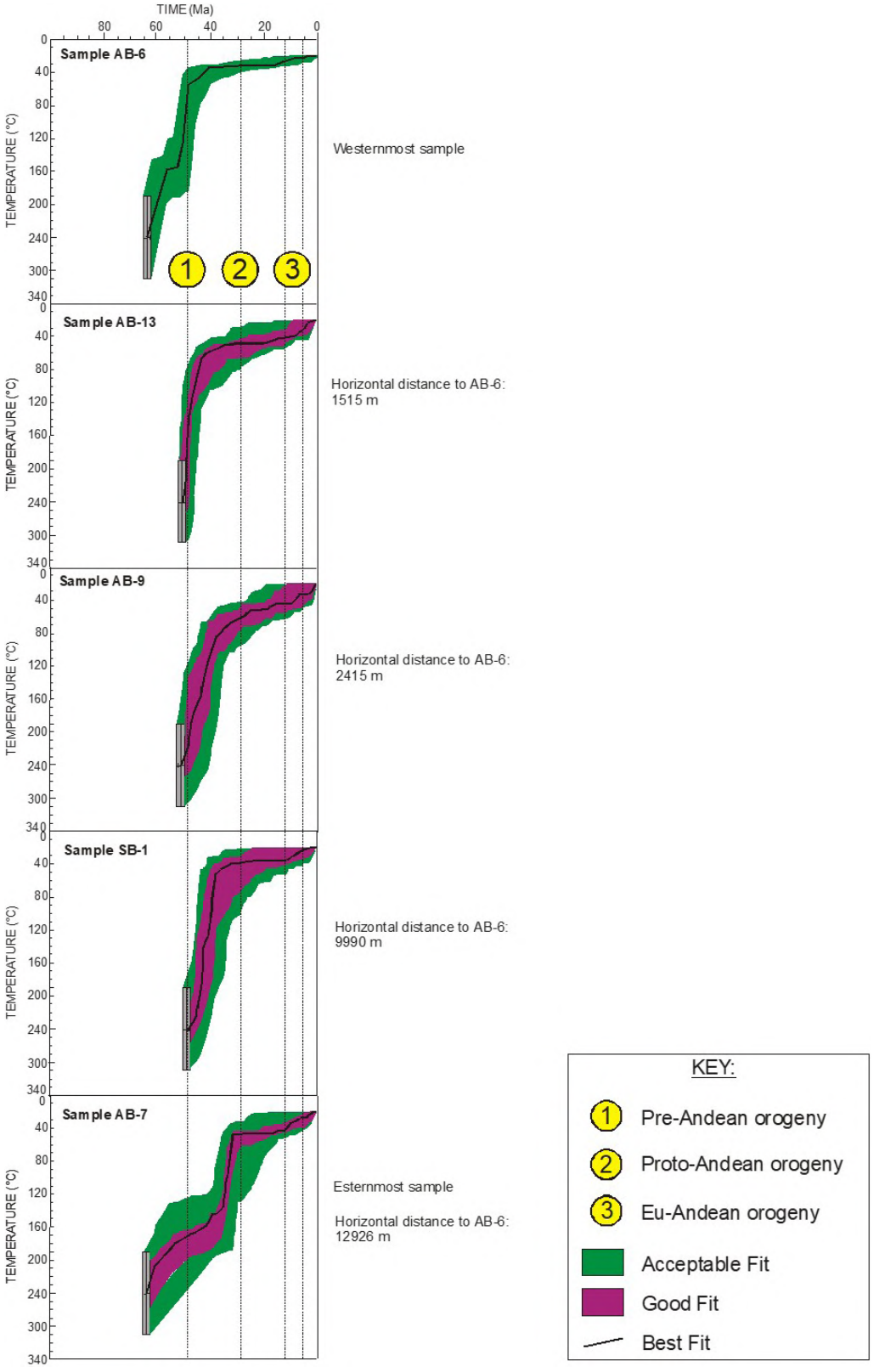

Figure 13. Relation between the generated t-T paths and the orogenic phases.

Comparison with subsequent work

The data obtained in this study are in reasonable agreement with two subsequent studies. Initially, using the same fission track methodology in Toro *et al.*, 2007, for whom the last uplift of the northern sector of the central Cordillera would be the kinematic response to the regional NWSE thrust, product of the Panama-Costa Rica Microplate and the Caribbean Plate interaction with the Andean Block, which according to their results began around 7 Ma, with a maximum activity between 3.6 and 3.1 Ma. Later, using apatite (U–Th)/He thermochronology (Restrepo-Moreno *et al.*, 2009) reveal two strong cooling events, one from 41 Ma to 49 Ma and the other between 21 Ma and 25 Ma. AHe data provide an average erosion rate of ~ 0.04 mm/yr for the last 25 million years. Erosion rates during the exhumation pulses were in the order of ~ 0.2–0.4 mm/yr.

Special attention should be directed to tectometamorphic events that may affect the thermochronometers and that are being reported by new data. For example, the morphotectonic paroxysm near the Oligo-Miocene transition reported by Restrepo-Moreno *et al.* (2009) and Noriega-Londoño *et al.* (2020). Additionally, exhumation might be understood as due to differential behavior between the blocks; for Noriega-Londoño *et al.* (2020) is key the role of the Espiritu Santo Fault in the Antioquia Eastern Massif.

Conclusions

The obtained Zircon FT dates show statistical homogeneity and independence from surface processes. Therefore, these data are interpreted as cooling ages, meaning the time at which the sample evaluated passed through its closure temperature, estimated to be about 240°±50°C. Zircon ages range from 46.4±1.1 Ma to 64.0±1.3 Ma.

The time-temperature cooling paths show strong correlation with the orogenic phases that built the Colombian Andes, especially to those occurred during the middle Eocene (Pre-Andean), and late Miocene to Pliocene (Eu Andean). An Oligocene phase (Proto-Andean) was not identified by this tool. The main tectonic phase that affected the study area occurred between the middle and late Eocene. After that, the present surface remained awfully quite close to the surface at that time (less than 1 km), until unroofing occurred during the late Miocene to Pliocene orogenic phase. The western samples cooled before the eastern ones during this well-identified orogenic phase, showing a clear eastward migration of the deformation front. This migration is evident in the stratigraphic record.

The samples were most likely exhumed between 3 and 5 Ma ago, although we must accept some statistical probability associated with the method up to 11Ma. This data represents the maximum age for the formation of the landscape as it was denuded to place the samples on surface; in other words, the Central Cordillera erosion surface and its superimposed relief were formed after this time.

Acknowledgments

This research is part of the author Edgar Saenz's thesis for his master's degree in science and engineering – geosciences, obtained at Shimane University of Matsue, Japan. This project was conducted with the support of the Japan-IBD scholarship program, and the supervision of all academic activity was carried out by Professor Hiroto Ohira. I am deeply thankful to him for his guidance, lessons, comments, and constructive criticism.

My acknowledgements to all the staff of the Geosciences Department of Shimane University, especially to Dr. Shigeru Iizumi and Dr. Akira Takasu. My deepest gratitude to Dr Barry Roser, who made essential suggestions.

I thank Dra. Gloria Toro access to using the laboratory facilities at EAFIT, and for her assistance and guidance during the first steps of the laboratory work.

This research was born from the Fission Tracks seed planted at the Universidad Nacional Medellín by professors José Maria Jaramillo and Jorge Julián Restrepo. Together with Carlos Paucar we did one of the first undergraduate thesis on the subject (Paucar and Saenz, 1995) under the direction of J.J. Restrepo and that was the beginning of this project.

Finally, thanks to Professor Sergio Restrepo who encouraged us to submit this article and contributed to our knowledge of advances in the Central Cordillera thermochronology.

References

Anderson, T.A. (1972). Paleogene nonmarine Gualanday Group, Neiva Basin, Colombia, and regional development of the Colombian Andes. *GSA Bulletin, 83*(8), 2423-2438. https://doi.org/10.1130/0016-7606(1972)83[2423:PNGGNB]2.0.CO;2

Arias-López, L.A. (1995). El relieve de la zona central de Antioquia: Un palimpsesto de eventos tectónicos y climáticos. *Revista Facultad de Ingeniería, Universidad de Antioquia, 10,* 9-24. https://doi.org/10.17533/udea.redin.325539

Aspden, J.A.; McCourt, W.J. (1986). Mesozoic oceanic terrane in the central Andes of Colombia. *Geology, 14*(5), 415-418. https://doi.org/10.1130/0091-7613(1986)14<415:MOTITC>2.0.CO;2

Aspden, J.A.; McCourt, W.J.; Brook, M. (1987). Geometrical control of subduction–related magmatism: The Mesozoic and Cenozoic plutonic history of Western Colombia. *Journal of the Geological Society, 144*(6), 893-905. https://doi.org/10.1144/gsjgs.144.6.0893

Botero-Arango, G. (1963). Contribución al conocimiento de la geología de la Zona Central de Antioquia. *Anales de la Facultad de Minas*, *57*.

Bourgois, J.; Toussaint, J.F.; González, H.; Azema, J.; Calle, B.; Desmet, A.; Murcia, L.A.; Acevedo, A.P.; Parra, E.; Tournon, J. (1987). Geological history of the Cretaceous ophiolitic complexes of northwestern South America (Colombian Andes). *Tectonophysics, 143*(4), 307-327. https://doi.org/10.1016/0040-1951(87)90215-0

Carlson, W.D.; Donelick, R.A.; Ketcham, R.A. (1999). Variability of apatite fission-track annealing kinetics: I. Experimental results. *American Mineralogist, 84*(9), 1213-1223. https://doi.org/10.2138/am-1999-0901

Correa, A.M.; Pimentel, M.; Restrepo, J.J.; Nilson, A.; Ordóñez, O.; Martens, U.; Laux, J.E.; Junges, S. (2006). U-Pb zircon ages and Nd-Sr isotopes of the Altavista Stock and the San Diego Gabbro: New insights on Cretaceous arc magmatism in the Colombian Andes. *V South American Symposium on Isotope Geology*, Punta del Este, Uruguay.

Donelick, R.A.; Ketcham, R.A.; Carlson, W.D. (1999). Variability of apatite fission-track annealing kinetics: II. Crystallographic orientation effects. *American Mineralogist*, *84*(9), 1224-1234. https://doi.org/10.2138/am-1999-0902

Dunkl, I. (2002). Trackkey: a Windows program for calculation and graphical presentation of fission track data. *Computers & Geosciences, 28*(1), 3-12. https://doi.org/10.1016/S0098-3004(01)00024-3

Duque-Caro, H. (1980). Geotectónica y evolución de la región noroccidental colombiana. *Boletín Geológico, 33*(3), 1-37. https://doi.org/10.32685/0120-1425/bolgeol23.3.1980.257

Duque-Caro, H. (1990). Neogene stratigraphy, paleoceceanography and paleobiogeography in northwest South America and the evolution of the Panama Seaway. *Palaeogeography, Palaeoclimatology, Palaeoecology, 77*(3-4), 203-234. https://doi.org/10.1016/0031-0182(90)90178-A

Feininger, T.; Botero, G. (1982). The Antioqueño Batholith, Colombia. *Publicaciones Geológicas Especiales del Ingeominas, 12*, 1-50.

Galbraith, R.F. (1981). On statistical models of fission track counts. *Journal of the International Association for Mathematical Geology, 13*(6), 471-478. https://doi.org/10.1007/BF01034498

Galbraith, R.F.; Laslett, G.M. (1993). Statistical models for mixed fission track ages. *Nuclear Tracks and Radiation Measurements, 21*(4), 459-470. https://doi.org/10.1016/1359-0189(93)90185-C

García-Casco, A.; Restrepo, J.J.; Correa-Martínez, A.M.; Blanco-Quintero, I.F.; Proenza, J.A.; Weber, M.; Butjosa, L. (2020). The petrologic nature of the "Medellín Dunite" revisited: An algebraic approach and proposal of a new definition of the geological body. In: J. Gómez, A.O. Pinilla-Pachon (eds.). *The Geology of Colombia* (pp. 45-75). Volume 2. Servicio Geológico Colombiano. https://doi.org/10.32685/pub.esp.36.2019.02

Gleadow, A.J.W.; Brown, R.W. (1999). Fission track thermochronology and the long-term denudational response to tectonics. In: M.A. Summerfield (eds.). *Geomorphology and Global Tectonics* (pp. 57-75). John Wiley and Sons Ltd.

Hermelin, M. (1982). El origen del Valle de Aburrá, evolución de las ideas. *Boletín de Ciencias de la Tierra, 7-8*, 47-65.

Hoorn, C.; Guerrero, J.; Sarmiento, G.A.; Lorente, M.A. (1995). Andean tectonics as a cause for changing drainage patterns in Miocene northern South America. *Geology, 23*(3), 237-240. https://doi.org/10.1130/0091-7613(1995)023%3C0237:ATAACF%3E2.3.CO;2

Hurford, A.J.; Green, P.F. (1983). The zeta age calibration of fission-track dating. *Chemical Geology, 41,* 285-317. https://doi.org/10.1016/S0009-2541(83)80026-6

Hurford, A.J. (1986). Cooling and uplift patterns in the Lepontine Alps south-central Switzerland and an age of vertical movement on the Insubric fault line. *Contributions to Mineralogy and Petrology, 92*(4), 413-427. https://doi.org/10.1007/BF00374424

Ibáñez-Mejía, M.; Restrepo, J.J.; García-Casco, A. (2020). Tectonic juxtaposition of Triassic and Cretaceous meta-(ultra)mafic complexes in the Central Cordillera of Colombia (Medellin area) revealed by zircon U-Pb geochronology and Lu-Hf isotopes. In: A. Bartorelli, W. Teixeira, B. Neves (eds.). *Geocronologia e Evolução Tectônica do Continente Sul-Americano: a contribuição de Umberto Giuseppe Cordani* (pp. 418-443). Solaris Edições Culturais.

Irving, E.M. (1975). Structural evolution of the northernmost Andes, Colombia. *U.S. Geological Survey Professional Paper, 846*, 1-47. https://doi.org/10.3133/pp846

Keller, G.; Barron, J.A. (1987). Paleodepth distribution of Neogene deep-sea hiatuses. *Paleoceanography and Paleoclimatology, 2*(6), 697-713. https://doi.org/10.1029/PA002i006p00697

Ketcham, R.A.; Donelick, R.A.; Carlson, W.D. (1999). Variability of apatite fission-track annealing kinetics: III. Extrapolation to geological time scales. *American Mineralogist, 84*(9), 1235-1255. https://doi.org/10.2138/am-1999-0903

Leal-Mejía, H. (2011). Phanerozoic gold metallogeny in the Colombian Andes: A tectono–magmatic approach. Doctorade thesis, Universitat de Barcelona, España.

Migon, P. (2006). Classic in Physical Geography Revisited. Büdel, J. (1982): Climatic geomorphology. Princeton: Princeton University Press. (Translation of Klima-geomorphologie, Berlin-Stuttgart: Gebrüder Borntraeger, 1977). *Progress in Physical Geography: Earth and Environment, 30*(1), 99-103. https://doi.org/10.1191/0309133306pp473xx

Montes-Correa L.F. (2007). Exhumación de las rocas metamórficas de alto grado que afloran al Oriente del Valle de Aburrá, Antioquia. Tesis de Maestría, Universidad EAFIT, Medellín, Colombia.

Noriega-Londoño, S. (2016). Geomorfología tectónica del noroccidente de la Cordillera Central, Andes del Norte-Colombia. Tesis de maestría, Universidad Nacional de Colombia, Medellin, Colombia.

Noriega-Londoño, S.; Restrepo-Moreno, S.A.; Vinasco, C.; Bermúdez, M.A.; Min, K. (2020). Thermochronologic and geomorphometric constraints on the Cenozoic landscape evolution of the Northern Andes: Northwestern Central Cordillera, Colombia. *Geomorphology, 351*, 106890. https://doi.org/10.1016/j.geomorph.2019.106890

Oppenheim, V. (1941). Geología de la Cordillera Oriental entre los Llanos y el Magdalena. *Revista de la Academia Colombiana de Ciencias Exactas, Físicas y Naturales, 4*(14), 175-181.

Ordóñez-Carmona, O.; Pimentel, M. (2001). Consideraciones geocronológicas e isotópicas del Batolito Antioqueño. *Revista de la Academia Colombiana de Ciencias Exactas, Físicas y Naturales, 25*(94), 27-35. https://doi.org/10.18257/raccefyn.25(94).2001.2710

Ordóñez-Carmona, O.; Pimentel, M.M.; Ángel-Cárdenas, P. (2001). Consideraciones geocronológicas e isotópicas preliminares del magmatismo Cretaceo-Paleoceno en el Norte de la Cordillera Central. *VIII Congreso Colombiano de Geología*, Manizales, Colombia.

Ordóñez, O.; Pimentel, M.M.; Laux, J.H. (2008). Edades U–Pb del Batolito Antioqueño. *Boletín de Ciencias de la Tierra, 22*, 129-130.

Page, W.D.; James, M.E. (1981). The antiquity of the erosion surfaces and late Cenozoic deposits near Medellín, Colombia: Implications to tectonics and erosion rates. *Revista CIAF, 6*(1-3), 421-454.

Paucar, C.; Saenz, E. (1995). Estudio de la evolución térmica del Batolito Antioqueño por huellas de fisión. Tesis de grado, Universidad Nacional de Colombia, Medellín, Colombia.

Pérez-Ángel, G. (1967). Determinación de edad absoluta de algunas rocas de Antioquia por métodos radioactivos. *Dyna, 84*, 27-31.

Rendón, D. (2003). Tectonic and sedimentary evolution of the Aburra Valley, northern Colombian Andes. Master Thesis, Shimane University, Matsue, Japan.

Restrepo, J.J.; Toussaint, J.F. (1982). Metamorfismos superpuestos de la Cordillera Central de Colombia. *V Congreso Latinoamericano de Geología,* Buenos Aires, Argentina.

Restrepo, J.J.; Toussaint, J.F. (1990). Cenozoic arc magmatism of northwestern Colombia. In: S.M. Kay, C.W. Rapela (eds.). *Plutonism from Antarctica to Alaska* (pp. 205-212). Geological Society of America. https://doi.org/10.1130/SPE241-p205

Restrepo, J.J.; Toussaint, J.F. (2020). Tectonostratigraphic terranes in Colombia: An update. First part: Continental terranes. In: J. Gómez, D. Mateus-Zabala (eds.). *The Geology of Colombia* (pp. 37-63). Volume 1. Servicio Geológico Colombiano. https://doi.org/10.32685/pub.esp.35.2019.03

Restrepo, J.J.; Frantz, J.C.; Ordóñez-Carmona, O.; Correa, A.M.; Martens, U.; Chemale, F. (2007). Edad triásica de formación de la Ofiolita de Aburrá, flanco occidental de la Cordillera Central. *XI Congreso Colombiano de Geología,* Bucaramanga, Colombia.

Restrepo, J.J.; Ordóñez-Carmona, O.; Armstrong, R.; Pimentel, M.M. (2011). Triassic metamorphism in the northern part of the Tahamí Terrane of the Central Cordillera of Colombia. *Journal of South American Earth Sciences, 32*(4), 497-507. https://doi.org/10.1016/j.jsames.2011.04.009

Restrepo-Moreno S.A. (2009). Long-term morphotectonic evolution and denudation chronology of the Antioqueño Plateau, Cordillera Central, Colombia. PhD Thesis, University of Florida, USA.

Restrepo-Moreno, S.A.; Foster, D.A.; Stockli, D.F.; Parra-Sánchez, L.N. (2009). Long-term erosion and exhumation of the "Altiplano Antioqueño", Northern Andes (Colombia) from apatite (U–Th)/He thermochronology. *Earth and Planetary Science Letters, 278*(1-2), 1-12. https://doi.org/10.1016/j.epsl.2008.09.037

Saenz, E. (2003). Fission track thermochronology and denudational response to tectonics in the north of the Colombian Central Cordillera. Master thesis. Shimane University, Matsue, Japan.

SIGAC (2017). Mapa digital, Departamento de Antioquia a escala 1:500.000. Instituto Geográfico Agustín Codazzi.

Steiger, R.H.; Jager, E. (1977). Subcommission on geochronology: convention on the use of decay constants in geo- and cosmochronology. *Earth and Planetary Science Letters, 36*(3), 359-362. https://doi.org/10.1016/0012-821X(77)90060-7

Suwa, K.; Enami, M.; Horiuchi, T. (1987). Chlorine-rich potassium hastingsite from West Ongul Island, Lützow–Holm Bay, East Antarctica. *Mineralogical Magazine, 51*(363), 709-714. https://doi.org/10.1180/minmag.1987.051.363.11

Toro, G.; Hermelin, M.; Schwave, E.; Posada, B.; Silva, D.; Poupeau, G. (2006). Fission-track datings and long-term stability in the Central Cordillera highlands, Colombia. In: E. Latrubesse (ed.). *Tropical Geomorphology with Special Reference to South America* (pp. 1-16).

Toro, G.E; Rendón. D.A.; Montes, L. (2007). Levantamiento de los Andes en el norte de la Cordillera Central de Colombia: una aproximación geomorfológica, estructural y cronológica (trazas de fisión). *Boletín de Ciencias de la Tierra, 22*, 125-126.

Toussaint, J.F.; Restrepo, J.J. (2020). Tectonostratigraphic terranes in Colombia: An update. Second part: Oceanic terranes. In: J. Gómez, A.O. Pinilla-Pachon (eds.). *The Geology of Colombia* (pp. 237-260). Volume 2. Servicio Geológico Colombiano. https://doi.org/10.32685/pub.esp.36.2019.07

Villagómez-Díaz, D. (2010). Thermochronology, geochronology and geochemistry of the Western and Central cordilleras and Sierra Nevada de Santa Marta, Colombia: the tectonic evolution of NW South America. PhD Thesis, Université de Genève, Switzerland.

Villagómez, D.; Spikings, R.; Magna, T.; Kammer, A.; Winkler, W.; Beltrán, A. (2011). Geochronology, geochemistry and tectonic evolution of the Western and Central cordilleras of Colombia. *Lithos, 125*(3-4), 875-896. https://doi.org/10.1016/j.lithos.2011.05.003

Villamil, T. (1999). Campanian–Miocene tectonostratigraphy, depocenter evolution and basin development of Colombia and western Venezuela. *Palaeogeography, Palaeoclimatology, Palaeoecology, 153*(1-4), 239-275. https://doi.org/10.1016/S0031-0182(99)00075-9

Van der Hammen, T. (1958). Estratigrafía del Terciario y Maestrichtiano continentales y tectogénesis de los Andes colombianos. *Boletín Geológico, 6*(1-3), 67-128. https://doi.org/10.32685/0120-1425/bolgeol6.1-3.1958.309

Vinasco, C.J.; Cordani, U.G.; González, H.; Weber, M.; Pelaez, C. (2006). Geochronological, isotopic and geochemical data from Permo-Triassic granitic gneisses and granitoids of the Colombian Central Andes. *Journal of South American Earth Sciences, 21*(4), 355-371. https://doi.org/10.1016/j.jsames.2006.07.007

Received: 31 May 2023
Accepted: 05 April 2024